

Anomalous quantum Hall states in an optical lattice

S. R. Hassan, Sandeep Goyal, R. Shankar

The Institute of Mathematical Sciences, C.I.T. Campus, Chennai 600 113, India

David Sénéchal

Département de Physique and RQMP, Université de Sherbrooke, Sherbrooke, Québec, Canada J1K 2R1

(Dated: January 30, 2012)

We analyze the Physics of cold atoms in honeycomb optical lattices with on-site repulsion and spin-orbit couplings that break time reversal symmetry. Such systems, at half filling and large on-site repulsion, have been proposed as a possible realization of the Kitaev model. The spin-orbit couplings break the spin degeneracy and, if strong-enough, lead to four non-overlapping bands in the non-interacting limit. These bands carry non-zero Chern number and therefore the non-interacting system has non-zero angular momentum and chiral edge states at $1/4$ and $3/4$ filling. We have investigated the effect of interactions using the variational cluster perturbation theory and conclude that the chiral edge states exist in finite range of interaction and hopping parameter space.

PACS numbers: 71.10.Fd, 73.43.-f

INTRODUCTION

Systems with topological quantum order have been of much interest recently. These systems are characterized by quasi-particles with fractional charge and statistics. Systems with non-Abelian statistics are especially interesting since they can be used for fault-tolerant quantum computation. The Kitaev model on the honeycomb lattice is a quantum spin- $\frac{1}{2}$ model that has such topological order [1]. There have been recent proposals [2–4] to realize this model in an optical lattice, using two-state bosonic or fermionic atoms with spin-dependent hopping on a honeycomb lattice with on-site repulsion. The Kitaev model is then the effective Hamiltonian at half-filling and large repulsion.

In this paper, we concentrate on the fermionic model defined on a honeycomb lattice. Let \mathbf{b}_a ($a = 1, 2, 3$) denote the vectors linking a site on the A sublattice with its three neighbors on the B sublattice, and let $\langle ij \rangle_a$ denote the nearest-neighbor pairs along these three directions. The Hamiltonian of the model is then

$$H = \sum_{\langle ij \rangle_a} \left\{ c_i^\dagger P^a c_j + \text{H.c.} \right\} + U \sum_i n_{i\uparrow} n_{i\downarrow} \quad (1)$$

where $P^a = \frac{1}{2}(t + t'\sigma^a)$ and σ^a are the Pauli matrices (we have suppressed the spin indices). The number of fermions at site i is $n_{i\sigma} = c_{i\sigma}^\dagger c_{i\sigma}$. At $t' = 0$, the model reduces to the simple spin-invariant, nearest-neighbor (NN) Hubbard model, as relevant to graphene, and is time-reversal invariant. At $t' = t$, the one-body part of the Hamiltonian is a combination of the projection operators $\frac{1}{2}(1 + \sigma^a)$. Thus, only electrons that are spin polarized in the a direction can hop along the a bonds. At this value of t' , at half filling and large U , the effective low energy spin model is the Kitaev honeycomb model [2–4].

The term proportional to t' is a spin-orbit coupling. It is qualitatively different from the usual spin-orbit term

as it breaks time reversal symmetry. The physical origin of this lies in the asymmetry of the laser beams coupling the two spin components to an excited level (which makes the potential barrier spin dependent). It is interesting to note that a time reversal invariant hopping term of the form $H = \sum_{\langle ij \rangle_a} \left(\frac{1}{2} c_i^\dagger (t + it'\sigma^a) c_j + \text{H.c.} \right)$ does not lead to the Kitaev model at half filling in the large- U limit.

Topological effects in electronic bands were highlighted in the seminal paper of Thouless *et al.* [5] where the quantized Hall conductivity was expressed as the sum of the Chern numbers of the occupied bands (when the Fermi level lies in a gap). The Chern number and hence the quantized Hall conductivity was later identified with the number of chiral edge channels at the Fermi level by Hatsugai [6]. A non-zero Chern number can only occur in a system which is not time reversal invariant. However, this does not necessitate an external magnetic field: Haldane constructed a tight-binding model on a honeycomb lattice with next-NN hopping terms that are not time reversal invariant [7]. In that model the two bands carry Chern numbers equal to ± 1 and an anomalous Hall effect occurs when the bands are partially filled [8]. The Hall conductivity is quantized when the Fermi level lies in the gap. More recently, the topology of time reversal invariant electronic bands with spin-orbit couplings has been extensively studied in the physical context of the spin Hall effect, leading to the discovery of topological insulators [9, 10]. The effect of time reversal breaking spin-orbit terms, to our knowledge, has not been studied so far.

In the rest of the paper, we concentrate on Model (1) at $\frac{1}{4}$ (or $\frac{3}{4}$) filling and show that it is in an anomalous quantized Hall state in a region of the $(t'-U)$ plane. At $U = 0$, the four bands carry Chern numbers equal to ± 1 . At large enough t' , they do not overlap, leading to quantized anomalous Hall states at fillings $\frac{1}{4}$ and $\frac{3}{4}$. We analyze the corresponding chiral edge state structure and

propose a way to detect them. We then study the model at $U > 0$ using Cluster Perturbation Theory [11] (CPT) and the Variational Cluster Approximation [12].

The model is easily diagonalized in the $U = 0$ limit. See Supplemental Material for details. The single-particle Hamiltonian in momentum space can be written as

$$h(\mathbf{k}) = \sum_k (\alpha^+ \otimes \Sigma(\mathbf{k}) + \alpha^- \otimes \Sigma^\dagger(\mathbf{k})) \quad (2)$$

where $\Sigma(\mathbf{k}) = P_3 + P_1 e^{ik_1} + P_2 e^{-ik_2}$, $k_{1,2}$ are the components of the lattice basis vectors $\mathbf{e}_{1,2}$, and α^\pm are the raising and lowering Pauli matrices acting on sublattice indices (A and B). The single-particle spectrum is completely determined in terms of the spectrum of the 2×2 positive semi-definite matrix, $\Sigma \Sigma^\dagger = \epsilon_0^2 + \frac{3}{4}(t')^2 + \frac{t'}{2} \mathbf{B} \cdot \boldsymbol{\sigma}$ where $\epsilon_0(\mathbf{k}) = \frac{1}{2}|(1 + e^{ik_1} + e^{-ik_2})|$ and

$$\begin{aligned} \mathbf{B} = & (1 - t' \sin k_1 + \cos k_2 + \cos k_3) \mathbf{b}_1 \\ & + (1 + \cos k_1 - t' \sin k_2 + \cos k_3) \mathbf{b}_2 \\ & + (1 + \cos k_1 + \cos k_2 - t' \sin k_3) \mathbf{b}_3 \end{aligned} \quad (3)$$

The energy spectrum of the four bands is $\epsilon(\mathbf{k})_{pp'} = p' (\epsilon_0^2(\mathbf{k}) + \frac{3}{4}(t')^2 + p \frac{1}{2} t' |\mathbf{B}|)^{\frac{1}{2}}$, where $p, p' = \pm 1$.

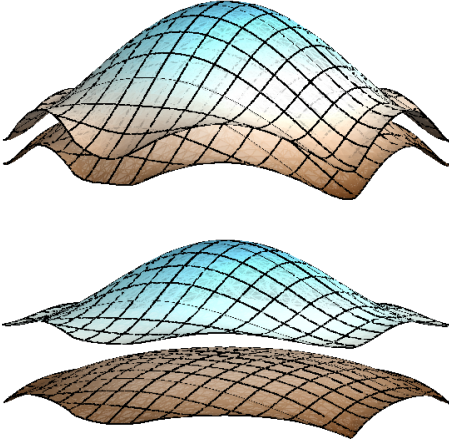


FIG. 1. (Color online) The two positive energy bands at $t' = 0.1$ (top) and $t' = 0.9$ (bottom). The negative energy bands are symmetrically located underneath the zero-energy plane and do not touch the upper bands. The two bands are overlapping at $t' = 0.1$ and well separated at $t' = 0.9$.

At $t' = 0$, we recover the graphene spectrum: The are two spin degenerate bands touching each other at two distinct Dirac points at the zone boundary. At any non-zero value of t' , the spin degeneracy is broken. Two of the bands, ϵ_{+-} and ϵ_{--} , continue to touch each other at two Dirac points whereas the other two develop a gap. The ϵ_{++} , ϵ_{+-} and ϵ_{-+} , ϵ_{--} bands overlap until a critical value t'_c of t' given by $\sqrt{6} - \sqrt{3} = 0.717$. For $t' > t'_c$, a finite gap appears. This is illustrated in Fig. 1.

At $t' = \sqrt{3}$, the middle two bands, ϵ_{+-} and ϵ_{--} , touch each other at $k = 0$. For $t' > \sqrt{3}$, the point of contact splits into six more Dirac points, for a total of eight Dirac points.

The Chern number for each band is $\pm\nu$, where ν is the winding number of the unit vector field $\hat{\mathbf{B}}$. It is not difficult to prove that $|\mathbf{B}| \neq 0$ for all points in the Brillouin zone, for any non-zero value of t' and hence ν is well defined. We have numerically computed ν to be 1. The highest and lowest energy bands with energies, $\pm\epsilon_+$, have Chern numbers +1 whereas the middle two bands with energies, $\pm\epsilon_-$, have Chern numbers -1.

When $t' > 0.717$ and the bands are non-overlapping, the half-filled state has total Chern number zero but the quarter and three-quarter filled states have Chern numbers equal to ± 1 respectively. These states are thus analogous to quantum Hall states with quantized Hall conductivity $\sigma_H = \pm 1$. At $t' < 0.717$, the bands overlap and at quarter filling the Fermi level passes through the $\epsilon_{-\pm}$ bands. The system is then analogous to an anomalous Hall conductor with the “Hall conductivity” equal to the Pancharatnam-Berry curvature integrated over the occupied states [8].

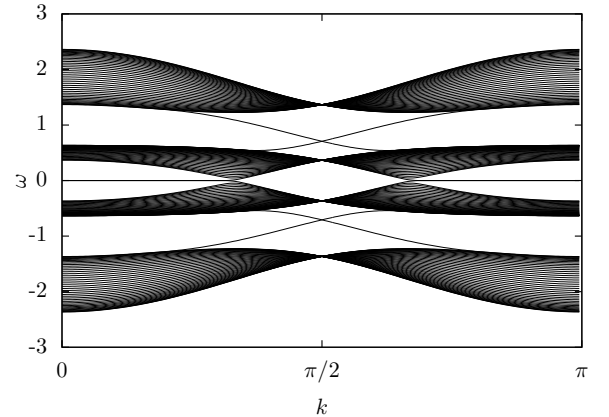


FIG. 2. The spectrum for an open tube of circumference $L = 60$ with zig-zag edges. Note the edge states that cross the gaps between the bands.

In the regime $t' > 0.717$, we expect chiral edge states in the gap between the $\epsilon_{+\pm}$ bands and also in the gap between the $\epsilon_{-\pm}$ bands. Our numerical calculations confirm this. Figure 2 shows the spectrum of the system with a cylindrical geometry and zig-zag edges. There are non-dispersive, zero energy edge states, as in graphene. There are also chiral edge states between the top two and the bottom two bands.

In a system of neutral atoms, the Hall conductivity is not easily measurable. However, the non-trivial topology also manifests itself in the orbital angular momentum, which is easier to measure then. The orbital magnetiza-

tion of Bloch electrons of the band pp' is given by [13–17]

$$\mathbf{M}_{pp'} = \frac{e}{2\hbar} \int_{p\epsilon_{p'}(\mathbf{k}) \leq \mu} \frac{d^2k}{(2\pi)^2} \times \langle \partial_{\mathbf{k}} \Phi^{pp'} | (H_{\mathbf{k}} + p\epsilon_{p'}(\mathbf{k}) - 2\mu) | \partial_{\mathbf{k}} \Phi^{pp'} \rangle, \quad (4)$$

where μ is the chemical potential (Fermi energy) and $|\Phi_{pp'}\rangle$ are the single particle eigenvectors. In the metallic case, Eq. (4) provides a μ -dependent magnetization, as it should. In the insulating case, when μ is varied in the gap, \mathbf{M} changes linearly only if the Chern invariant is non-zero, and remains constant otherwise. Eq. (4) is related – though not identical – to the anomalous Hall conductivity.

We computed the orbital magnetization as a function of the filling n by Eq. (4) in the metallic region at $t' = 0.5$ and in the insulating region at $t' = 1.0$. The behaviour of the orbital magnetization as the Fermi energy varies from the bottom of the lowest band to the top of the second band is displayed in Fig. 3. The orbital magnetization in the insulating phase at $t' = 1$ shows a discontinuity at $n = 0.25$, because the integral of the Pancharatnam-Berry curvature over the Brillouin zone is non-zero and quantized. The anomalous quantized Hall conductivity is the ratio of the discontinuity in the orbital magnetization to $E_g/(2e)$, where E_g is the gap between the first and the second band.

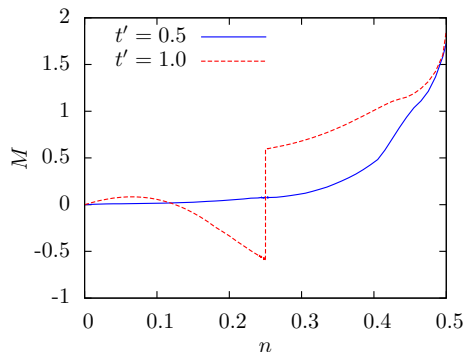


FIG. 3. (Color online) Orbital magnetization of the model as a function of the filling n for $t'=0.5, 1.0$

Thus far, the calculations we have presented were obtained in the non-interacting limit ($U = 0$). We now study the model as a function of the Hubbard interaction U to determine the region in the parameter space ($t' - U$) where the topological effects persist. The definition of the Chern invariant can be generalized to interacting systems in terms of the one-particle Green's function (see, e.g., Eq. (66) of Ref. [18]). It is expected to remain invariant provided the interaction does not close the gap and introduce new poles in the Green's function. It will also manifest itself as chiral edge states in the interacting system. We therefore address two questions: What is the region of parameter space where the gap persists? Are there chiral edge states in that region?

We study the interacting theory using Cluster Perturbation Theory [11] (CPT) and the Variational Cluster Approximation [12]. See Supplemental Material for a brief review of the technique.

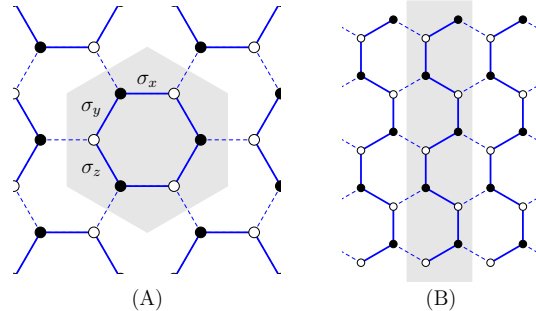


FIG. 4. (Color online) Clusters used in this work. Left: 6-site cluster used for the two-dimensional model. Right: 10-site cluster used for one-dimensional zigzag ribbons. Intercluster links are represented by dashed lines and the repeated unit is shaded in gray.

We have applied the VCA to the current system by treating the cluster spin magnetization M_c and the cluster chemical potential μ_c as variational parameters. Fig. 4 illustrates the clusters that were used in this work. Allowing μ_c to be different from μ and adopting the value that makes the Potthoff functional $\Omega(M_c, \mu_c)$ stationary ensures thermodynamic consistency, i.e., that the electron density n calculated from the CPT Green function coincides with $-\partial\Omega/\partial\mu$ [19]. This procedure allows us to calculate a more accurate value of the electron density n , compared with the simple CPT result.

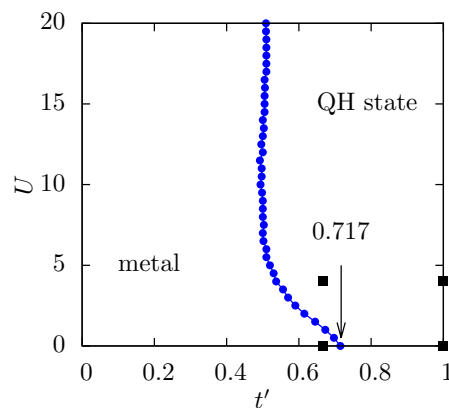


FIG. 5. (Color online). The phase diagram of the model in U - t' plane.

We have scanned several values of the interaction U and of the spin-orbit coupling t' , in order to find whether the system remains gapped at quarter-filling. Fig. 5 shows the phase diagram thus obtained, on the $t' - U$ plane. The curve shown is the phase boundary, i.e., the critical value t'_c at which the Fermi energy moves from the

gap to within the band, as a function of U . In the insulating region (right) the system remains in the quantum Hall state. Left of the line, the gap disappears and the system becomes metallic. We call this a *chiral metal* because non quantized Hall current flows along its boundary. We conclude that the topology of the band is protected for $U > 0$, and that a gapped state exists for $t' \gtrsim 0.5$ if U is large enough.

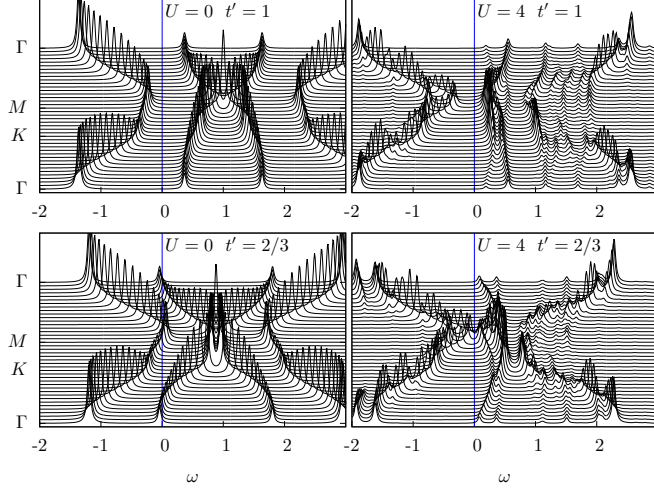


FIG. 6. Top: Single particle spectral function, as a function of ω , for spin-up electrons and wavevectors along high-symmetry directions at $t' = 1$ and $U = 0, 4$. Bottom: the same, at $t' = 2/3$. In all cases the system is quarter filled.

Fig. 6 displays the single-particle spectral weight $A_{\uparrow}(\mathbf{k}, \omega)$ of up-spins, as a function of frequency for wavevectors \mathbf{k} along high-symmetry directions. Three of the four plots are taken from the gapped phase, and one (bottom left) from the metallic phase. Although the gap is small at $U = 4$ and $t' = 2/3$ (bottom right), it is still nonzero. A Lorentzian broadening of $\eta = 0.03t$ has been used to make these plots, but the phase diagram itself was obtained by using several values of η and extrapolating the density of states towards $\eta = 0$.

We also calculated the spectral weight of zigzag ribbons of width 10 at $t' = 1$ and quarter filling. The system is shown on Fig. 4(B) and the spectral weight on Fig. 7. The bottom four bands are nearly degenerate at $k = \pi$ in the presence of interactions and are still clearly separated from the chiral edge state (shown by the red arrow) near that wavevector. This indicates that the chiral edge state persists at $U > 0$: the interaction does not destroy the topology of the bands.

In conclusion, we have shown that time reversal breaking spin-orbit interactions, in a model that can be realized in fermionic cold atom systems [2–4], lead to anomalous quantum Hall states at $\frac{1}{2}$ and $\frac{3}{4}$ filling. These states are robust against interactions and have a clear experimental signature, if the orbital angular momentum can be measured. Our result motivates the search for frac-

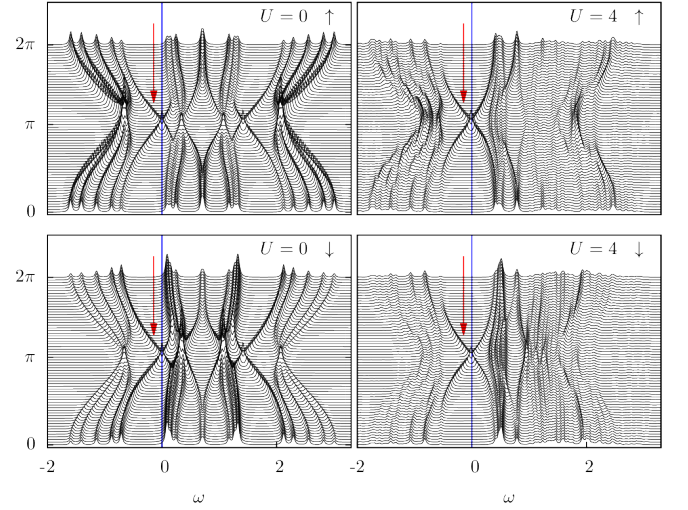


FIG. 7. (Color online) Top: Single particle spectral function of zigzag ribbons of 10 sites, as a function of energy ω . Top: up spins; bottom: down spins.

tional anomalous quantum Hall states in this model when the bands are partially filled. Work in this direction is in progress.

We are grateful to G. Baskaran, H.R. Krishnamurthy and A.-M.S. Tremblay for useful discussions. Computational resources were provided by Compute Canada and Calcul Québec.

SUPPLEMENTARY MATERIAL

Diagonalisation at $U = 0$

In this section we describe the details of the diagonalization of the model in the $U = 0$ limit. We label sites by (i_1, i_2, α) where $\alpha = 1, 2$ labels the sublattice. The unit cell positions span a triangular lattice and are given by $i_1 \hat{\mathbf{e}}_1 + i_2 \hat{\mathbf{e}}_2$, where the basis vectors are taken to be $\hat{\mathbf{e}}_{1(2)} = (\mp \frac{3}{2}, \frac{\sqrt{3}}{2})$.

We define the Fourier transform

$$c_{\mathbf{k}\alpha\sigma} = \sum_{i_1, i_2} e^{i\mathbf{k} \cdot (i_1 \hat{\mathbf{e}}_1 + i_2 \hat{\mathbf{e}}_2)} c_{i_1, i_2, \alpha, \sigma} \quad (5)$$

Let $P_a = \frac{1}{2}(1 + t' \sigma_a)$ and $k_{1(2)} \equiv \mathbf{k} \cdot \hat{\mathbf{e}}_{1(2)}$. The Hamiltonian in momentum space can then be written as ($t = 1$),

$$H = \sum_{\mathbf{k}} \begin{pmatrix} c_{\mathbf{k},1}^\dagger & c_{\mathbf{k},2}^\dagger \end{pmatrix} \begin{pmatrix} 0 & \Sigma(\mathbf{k}) \\ \Sigma^\dagger(\mathbf{k}) & 0 \end{pmatrix} \begin{pmatrix} c_{\mathbf{k},1} \\ c_{\mathbf{k},2} \end{pmatrix} \quad (6)$$

where $\Sigma(\mathbf{k}) = P_3 + P_1 e^{ik_1} + P_2 e^{-ik_2}$. We define α^x and α^y to be the two Pauli matrices with sublattice indices. Further defining $\alpha^\pm = (\alpha^x \pm i\alpha^y)/2$ the single particle hamiltonian can be written as,

$$h(\mathbf{k}) = \alpha^+ \otimes \Sigma(\mathbf{k}) + \alpha^- \otimes \Sigma^\dagger(\mathbf{k}) \quad (7)$$

The single-particle spectrum is completely determined in terms of the spectrum of the positive semi-definite matrix

$$\Sigma \Sigma^\dagger = f^* f + \frac{3}{4}(t')^2 + \frac{t'}{2} \mathbf{B} \cdot \boldsymbol{\sigma} \quad (8)$$

where

$$\begin{aligned} f &= \frac{1}{2}(1 + e^{ik_1} + e^{-ik_2}) \quad \text{and} \\ \mathbf{B} &= (1 - t' \sin k_1 + \cos k_2 + \cos k_3) \mathbf{b}_1 \\ &\quad + (1 + \cos k_1 - t' \sin k_2 + \cos k_3) \mathbf{b}_2 \\ &\quad + (1 + \cos k_1 + \cos k_2 - t' \sin k_3) \mathbf{b}_3 \end{aligned} \quad (9)$$

If $\phi^\pm(\mathbf{k})$ are the eigenvectors of $\mathbf{B}(\mathbf{k}) \cdot \boldsymbol{\sigma}$, with eigenvalues $\pm |\mathbf{B}(\mathbf{k})|$, then they are also the eigenvectors of $\Sigma(\mathbf{k}) \Sigma^\dagger(\mathbf{k})$ with eigenvalues,

$$\epsilon_\pm^2(\mathbf{k}) = f^* f + \frac{3}{4}(t')^2 \pm \frac{t'}{2} |\mathbf{B}(\mathbf{k})| \quad (10)$$

The four-component vectors

$$\Phi^{\pm\pm}(\mathbf{k}) = \frac{1}{\sqrt{2}} \begin{pmatrix} \phi^\pm(\mathbf{k}) \\ \pm \phi^\pm(-\mathbf{k}) \end{pmatrix} \quad (11)$$

are then the eigenvectors of the single-particle Hamiltonian defined by Eq. (6) with eigenvalues $\pm \epsilon_\pm(\mathbf{k})$.

The Chern numbers

The Pancharatnam-Berry curvature for each band is given by

$$\text{PB}^{pp'}(\mathbf{k}) = \frac{\epsilon_{ij}}{8\pi i} \left(\partial_i \Phi^{pp'}(\mathbf{k})^\dagger \partial_j \Phi^{pp'}(\mathbf{k}) - \text{H.c.} \right) \quad (12)$$

From Eq. (11) it is clear that

$$\begin{aligned} \text{PB}^{pp'}(\mathbf{k}) &= p' \frac{1}{2} (b(\mathbf{k}) + b(-\mathbf{k})) \\ b(\mathbf{k}) &= \frac{\epsilon_{ij}}{8\pi} \hat{\mathbf{B}}(\mathbf{k}) \cdot \partial_i \hat{\mathbf{B}}(\mathbf{k}) \times \partial_j \hat{\mathbf{B}}(\mathbf{k}) \end{aligned} \quad (13)$$

It is not difficult to prove that $|\mathbf{B}| \neq 0$ for all points in the Brillouin zone, *including the Dirac points*, for any non-zero value of t' . Thus $\text{PB}^{pp'}(\mathbf{k})$ is well defined throughout the Brillouin zone. We have numerically computed $\int_{\mathbf{k}} b(\mathbf{k})$ to be 1. Thus the Chern number of band pp' is p' : The highest and lowest energy bands, ϵ_{++} , have Chern numbers +1 whereas the middle two bands, ϵ_{+-} , have Chern numbers -1.

In the presence of interactions, the Chern number may still be calculated in principle, using the following expression [18]:

$$N = \frac{1}{24\pi^2} \int d^3k \epsilon^{\mu\nu\lambda} \text{tr} \{ G \partial_\mu G^{-1} G \partial_\nu G^{-1} G \partial_\lambda G^{-1} \} \quad (14)$$

where G stands for the Green function, the integral is taken over frequency and momentum and the trace is taken over spin and band indices. Greek indices are space-time indices running from 0 to 2. In the non-interacting case, this expression coincides with the integral of the Pancharatnam-Berry curvature over occupied states of the Brillouin zone. In the interacting case, the Green function will be deformed, but as long as a gap persists at the Fermi level, the Chern number should not be affected, as it is robust against smooth deformations that do not introduce or remove any poles in G .

CPT and VCA

CPT is an approximation scheme for the one-electron Green function $\mathbf{G}(\omega)$ within Hubbard-like models.[11, 20, 21] It proceeds by dividing the infinite lattice γ into a superlattice Γ of identical clusters of L sites each. The lattice Hamiltonian H is written as $H = H_c + H_T$, where H_c is the cluster Hamiltonian, obtained by severing the hopping terms between different clusters, which are put into H_T . If \mathbf{T} is the matrix of inter-cluster hopping terms and $\mathbf{G}^c(\omega)$ the exact Green function of the cluster. Because of the periodicity of the superlattice, \mathbf{T} can be expressed as a function of the reduced wavevector $\tilde{\mathbf{k}}$ and as a matrix in site indices within the cluster: $T_{ab}(\tilde{\mathbf{k}})$. Likewise, \mathbf{G}^c is a matrix in cluster site indices only, since all clusters are

identical: $G_{ab}^c(\omega)$. Thus, hopping matrices and Green functions in what follows will be $\tilde{\mathbf{k}}$ -dependent matrices of order L , the number of sites within each cluster. The fundamental result of CPT is

$$\mathbf{G}^{-1}(\tilde{\mathbf{k}}, \omega) = \mathbf{G}^{c-1}(\omega) - \mathbf{T}(\tilde{\mathbf{k}}) \quad (15)$$

In practice $\mathbf{G}^c(\omega)$ is calculated numerically by the Lanczos method and the cluster must be small enough for this to be possible. Because the lattice tiling breaks the original translation invariance of the lattice, a prescription is needed to restore the translation invariance of the resulting Green function. The CPT prescription for this periodization is

$$G(\mathbf{k}, \omega) = \frac{1}{L} \sum_{a,b} e^{-i(\mathbf{k}) \cdot (\mathbf{r}_a - \mathbf{r}_b)} G_{ab}(\mathbf{k}, \omega) \quad (16)$$

where now \mathbf{k} belongs to the Brillouin zone of the original lattice. This formula is exact in both the strong ($t \rightarrow 0$) and the weak ($U \rightarrow 0$) coupling limits.

Once the approximate interacting Green function can be calculated, various quantities can be calculated, such as the electron density $n(\mu)$ as a function of chemical potential, or the spectral function $A(\mathbf{k}, \omega)$ and its integral over wavevectors, the density of states $N(\omega)$.

The Variational Cluster Approximation (VCA) is an extension of CPT in which parameters of the cluster Hamiltonian H_c may be treated variationally, according to Potthoff's Self-Energy Functional Theory (SFT) [12, 22]. In particular, it allows the emergence of spontaneously broken symmetries and provides an approximate value for the system's grand potential Ω . Technically, VCA proceeds by minimizing the following quantity:

$$\Omega(h) = \Omega_c(h) - \int \frac{d\omega}{\pi} \frac{d^2k}{(2\pi)^2} \sum_{\tilde{\mathbf{k}}} \ln \det \left[\mathbf{1} - \mathbf{T}(\tilde{\mathbf{k}}) \mathbf{G}(\tilde{\mathbf{k}}, i\omega) \right] \quad (17)$$

where $\Omega_c(h)$ is the grand potential of the cluster alone (obtained in the exact diagonalization process). The integral over frequencies is carried over the positive imaginary axis, and h denotes collectively the parameters of the cluster Hamiltonian H_c that are treated variationally; these must be the coefficients of one-body operators. At the optimal value h^* , $\Omega(h^*)$ is the best estimate of the system's grand potential; in particular, its derivative

$\partial\Omega/\partial\mu = -n$ gives us a reliable estimate of the electron density. VCA provides estimates of order parameters, much like mean-field theory, but is quite superior to it because the Hamiltonian remains fully interacting (no factorization of the interaction) and spatial correlations are treated exactly within the cluster.

-
- [1] A. Kitaev, *Annals of Physics*, **321**, 2 (2006).
 - [2] L.-M. Duan, E. Demler, and M. D. Lukin, *Phys. Rev. Lett.*, **91**, 090402 (2003).
 - [3] C. Zhang, V. W. Scarola, S. Tewari, and S. Das Sarma, *Proceedings of the National Academy of Sciences*, **104**, 18415 (2007).
 - [4] R. Jördens, N. Strohmaier, K. Günter, H. Moritz, and T. Esslinger, *Nature*, **455**, 204 (2008).
 - [5] D. J. Thouless, M. Kohmoto, M. P. Nightingale, and M. den Nijs, *Phys. Rev. Lett.*, **49**, 405 (1982).
 - [6] Y. Hatsugai, *Phys. Rev. Lett.*, **71**, 3697 (1993).
 - [7] F. D. M. Haldane, *Phys. Rev. Lett.*, **61**, 2015 (1988).
 - [8] F. D. M. Haldane, *Phys. Rev. Lett.*, **93**, 206602 (2004).
 - [9] M. Z. Hasan and C. L. Kane, *Rev. Mod. Phys.*, **82**, 3045 (2010).
 - [10] X.-L. Qi and S.-C. Zhang, *Rev. Mod. Phys.*, **83**, 1057 (2011).
 - [11] D. Sénéchal, D. Perez, and M. Pioro-Ladrière, *Phys. Rev. Lett.*, **84**, 522 (2000).
 - [12] M. Potthoff, *Eur. Phys. J. B*, **32**, 429 (2003).
 - [13] J. Shi, G. Vignale, D. Xiao, and Q. Niu, *Phys. Rev. Lett.*, **99**, 197202 (2007).
 - [14] D. Xiao, M.-C. Chang, and Q. Niu, *Rev. Mod. Phys.*, **82**, 1959 (2010).
 - [15] D. Xiao, J. Shi, and Q. Niu, *Phys. Rev. Lett.*, **95**, 137204 (2005).
 - [16] T. Thonhauser, D. Ceresoli, D. Vanderbilt, and R. Resta, *Phys. Rev. Lett.*, **95**, 137205 (2005).
 - [17] D. Xiao, Y. Yao, Z. Fang, and Q. Niu, *Phys. Rev. Lett.*, **97**, 026603 (2006).
 - [18] G. Volovik, *Physics Reports*, **351**, 195 (2001).
 - [19] M. Aichhorn, E. Arrigoni, M. Potthoff, and W. Hanke, *Phys. Rev. B*, **74**, 235117 (2006).
 - [20] D. Sénéchal, D. Perez, and D. Plouffe, *Phys. Rev. B*, **66**, 075129 (2002).
 - [21] D. Sénéchal, in *Theoretical methods for Strongly Correlated Systems*, Springer Series in Solid-State Sciences, Vol. 171, edited by A. Avella and F. Mancini (Springer, 2012) Chap. 8, pp. 237–269.
 - [22] M. Potthoff, in *Theoretical methods for Strongly Correlated Systems*, Springer Series in Solid-State Sciences, Vol. 171, edited by A. Avella and F. Mancini (Springer, 2012) Chap. 9.